

Supplementary Materials for
**Identification of IgA autoantibodies targeting mesangial cells redefines the
pathogenesis of IgA nephropathy**

Yoshihito Nihei *et al.*

Corresponding author: Daisuke Kitamura, kitamura@rs.tus.ac.jp; Yusuke Suzuki, yusuke@juntendo.ac.jp

Sci. Adv. **9**, eadd6734 (2023)
DOI: 10.1126/sciadv.add6734

The PDF file includes:

Figs. S1 to S13
Tables S1 to S3
Legend for supplementary auxiliary files

Other Supplementary Material for this manuscript includes the following:

Supplementary auxiliary files

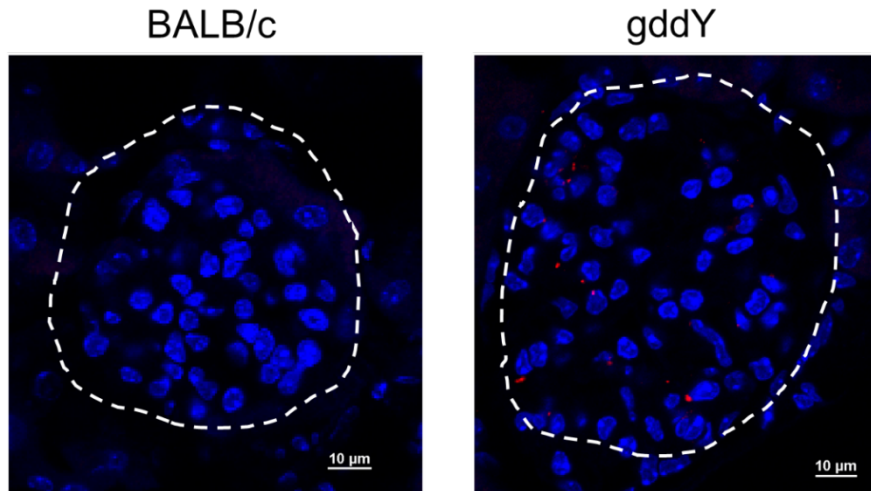


Fig. S1. Reactivity to glomeruli of purified serum IgA from gddY mice

Serum IgA was purified from 20-week-old (wo) BALB/c or gddY mice. Kidney sections from AID-knockout mice were stained with the purified IgA (10 µg/ml) from BALB/c (left) or gddY (right) mice, and secondarily with PE-anti-IgA Ab (red) with DAPI (blue). Dashed circles indicate areas of glomeruli.

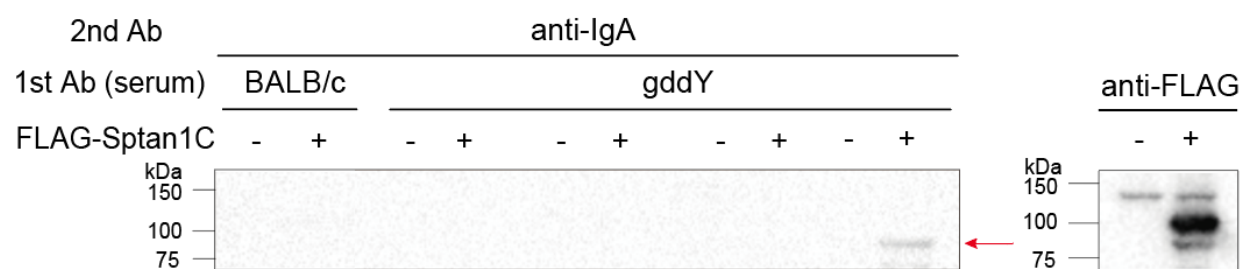


Fig. S2. Reactivity to α II-spectrin by the serum IgA of gddY mice

A representative WB of HEK293T cells transfected with a mock (-) or FLAG-tagged Sptan1C (+) vectors and probed with pooled sera from four 16-wk BALB/c mice or sera from gddY mice (n=4) followed by anti-IgA Ab (left). The red arrow indicates a band of Sptan1C, as confirmed with an anti-FLAG Ab (right). Shown is a representative of four independent experiments with different samples.

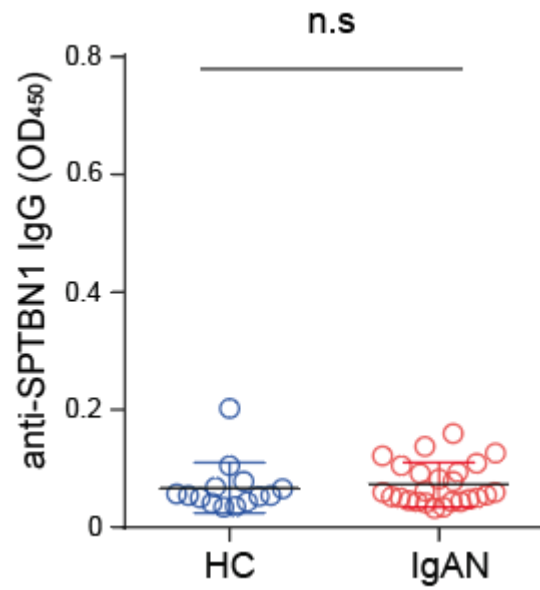


Fig. S3. Serum anti-SPTBN1 IgG levels in HC and IgAN patients

ELISA determination of anti-SPTBN1 IgG Abs in the same serum samples as in Fig. 2E were determined by ELISA. Small horizontal lines indicate the mean (black) \pm s.d. (colored) of each group. n. s: not significant.

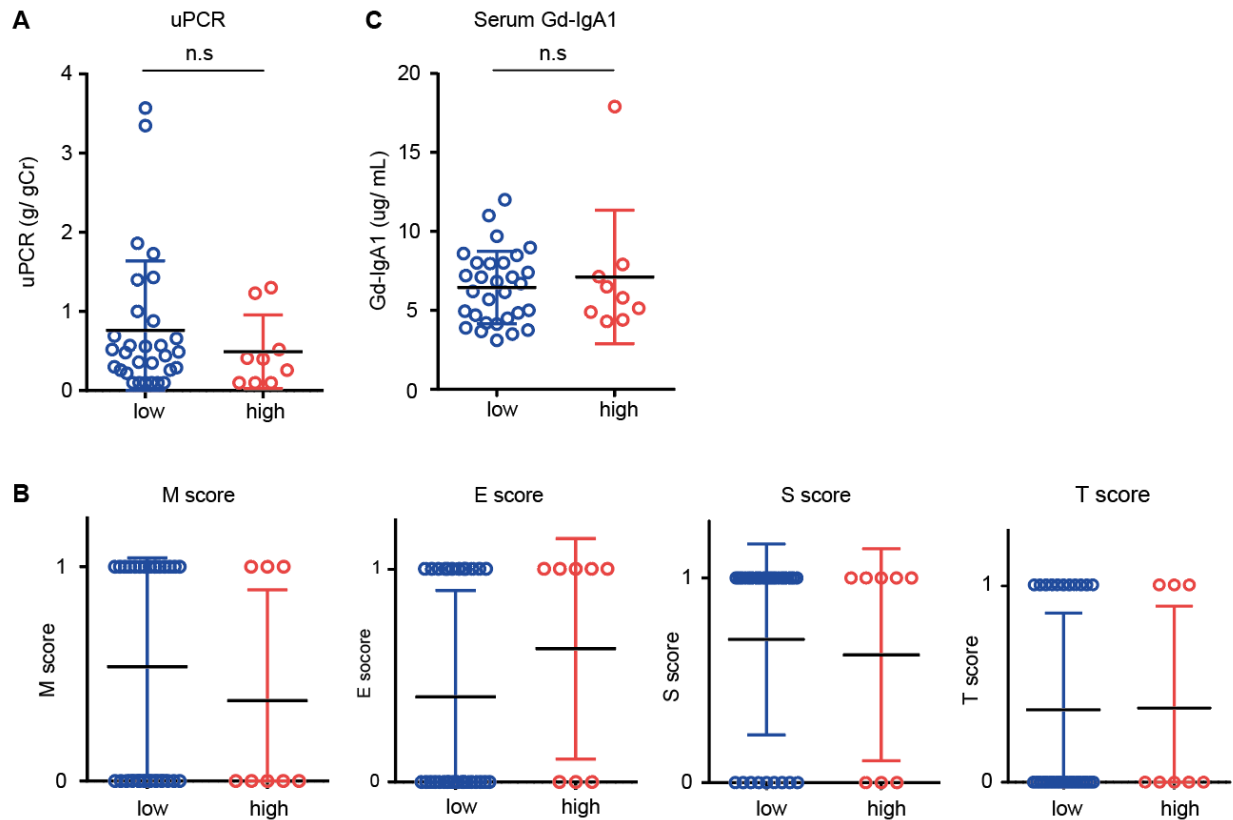


Fig. S4. Comparison of clinical and pathological parameters between anti-SPTBN1 IgA low and high groups of IgAN patients

(A to C) The levels of proteinuria (uPCR: urinary protein-to-creatinine ratio; A), MEST pathological scores (B) or serum Gd-IgA1 levels (C) were compared between the anti-SPTBN1 IgA ‘low’ (low) and ‘high’ (high) groups of IgAN patients. Small horizontal lines indicate the mean (black) \pm s.d. (colored) of each group. n. s.: not significant.

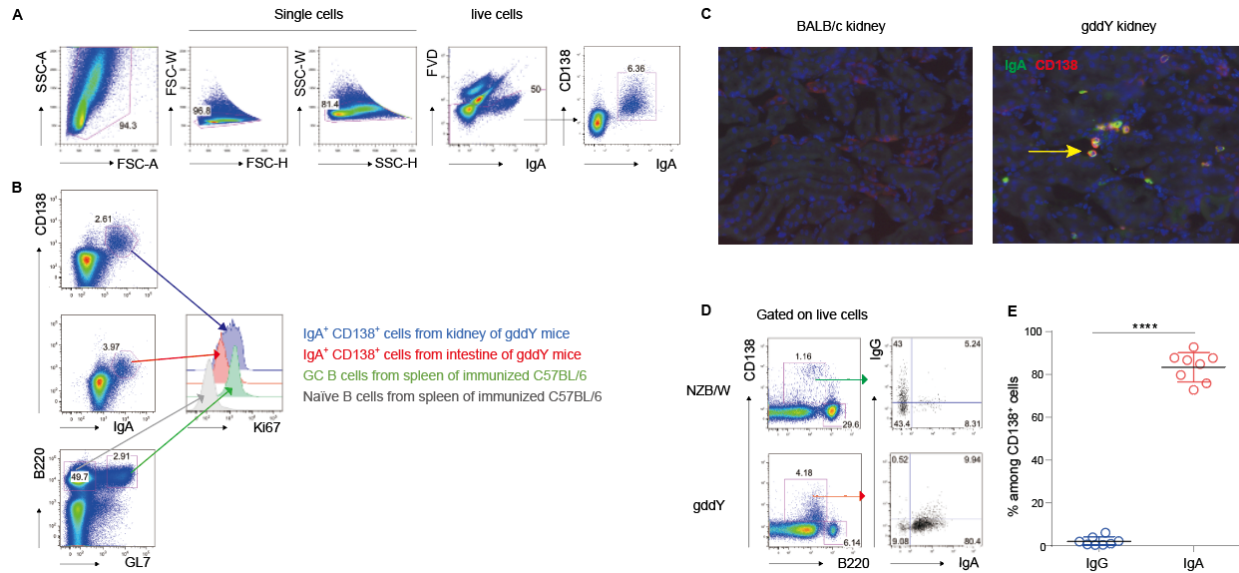


Fig. S5. IgA⁺ plasmablast accumulation in the kidney of gddY mice

(A) Gating strategy of IgA⁺ CD138⁺ plasmablasts (PBs) in the kidney of gddY mice.

(B) Flow cytometric analysis of Ki67 expression in the cells in the indicated gates. Shown here are histograms of IgA⁺ CD138⁺ cells in the kidney (blue) or the small intestine (red) of gddY mice, or B220⁺ GL7⁺ GC B cells (green) and B220⁺ GL7⁻ naïve B cells (gray) from the spleen of C57BL/6 mice immunized with NP-CGG in alum six days previously.

(C) Immunofluorescence microscopy of kidney sections of BALB/c or gddY mice stained for IgA (green) and CD138 (red), and with DAPI (blue). The arrow indicates one of the IgA⁺ CD138⁺ cells.

(D) Flow cytometric analysis of leukocytes from the kidneys of NZB/W F1 (top) and gddY (bottom) mice. CD138⁺ B220^{low} cells (left) were further analyzed for intracellular staining with anti-IgA and anti-IgG antibodies (right).

(E) The frequency of IgG⁺ (blue) or IgA⁺ (red) cells among the CD138⁺ B220^{low} cells in the kidneys of gddY mice as determined in (D) (n=8). Small horizontal lines indicate the mean (black) ± s.d. (colored) of each group. *****P* < 0.0001 (Student's *t*-test). The numbers in the panels indicate the percentage of cells within the adjacent gates among live cells (A, B and D) or within the quadrants (D).

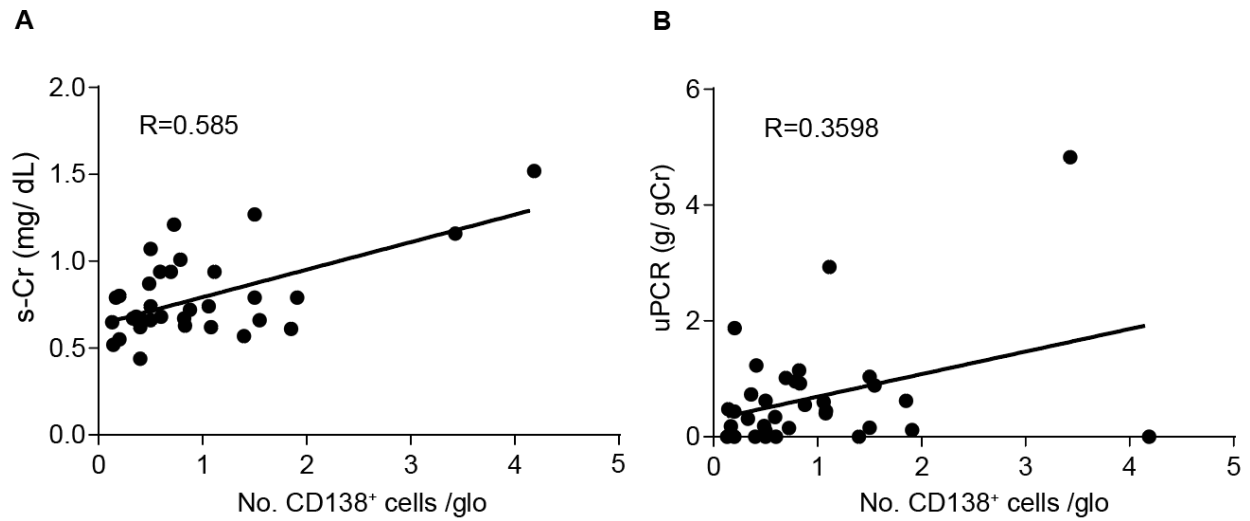


Fig. S6. Correlation between the frequency of IgA⁺ ASCs in the kidneys and disease severity in IgAN patients

(A and B) Serum creatinine levels (s-Cr; A) and the levels of proteinuria (uPCR; B) of the patients are plotted against the average number of CD138⁺ cells per glomeruli (CD138⁺ cells /glo) in biopsy samples of the same patients.

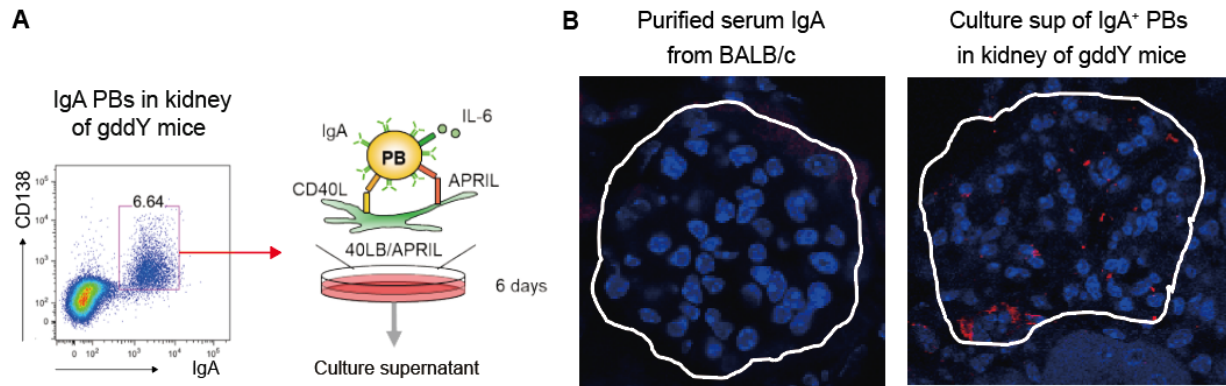


Fig. S7. Reactivity to glomerulus of IgA secreted by IgA⁺ PBs of the kidney in gddY mice

(A) Schematic representation of the culture system to produce Ab from PBs. IgA⁺ PBs sorted from the kidneys of gddY mice were cultured with IL-6 on 40LB/APRIL feeder cells for six days.

(B) Immunofluorescence microscopy of kidney sections of an AID-knockout mouse stained with serum IgA from 12-week-old BALB/c mice (control) or the supernatant of the culture described in (A), followed by PE-anti-IgA Ab (red) and DAPI (blue). White lines represent areas of the glomeruli.

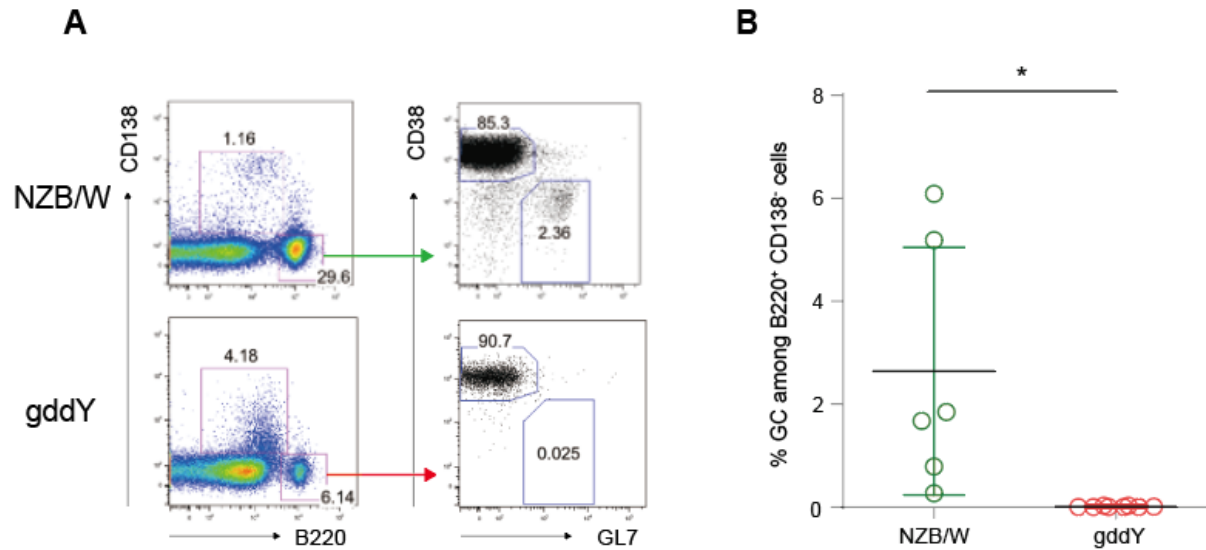


Fig. S8. Absence of GC B cells in the kidneys of 8-week-old gddY mice

(A) Flow cytometric analysis for the expression of GL7 and CD38 (right panels) on B220⁺ CD138⁻ cells (left panels) in the same samples as in fig. S5D.

(B) The frequency of GL7⁺ CD38⁻ (GC) B cells among B220⁺ CD138⁻ cells as determined in (A) (n=6 for NZB/W F1, n=8 for gddY). Small horizontal lines indicate the mean (black) ± s.d. (colored) of each group. * $P < 0.05$ (Student's *t* test). Data are representative of three independent experiments.

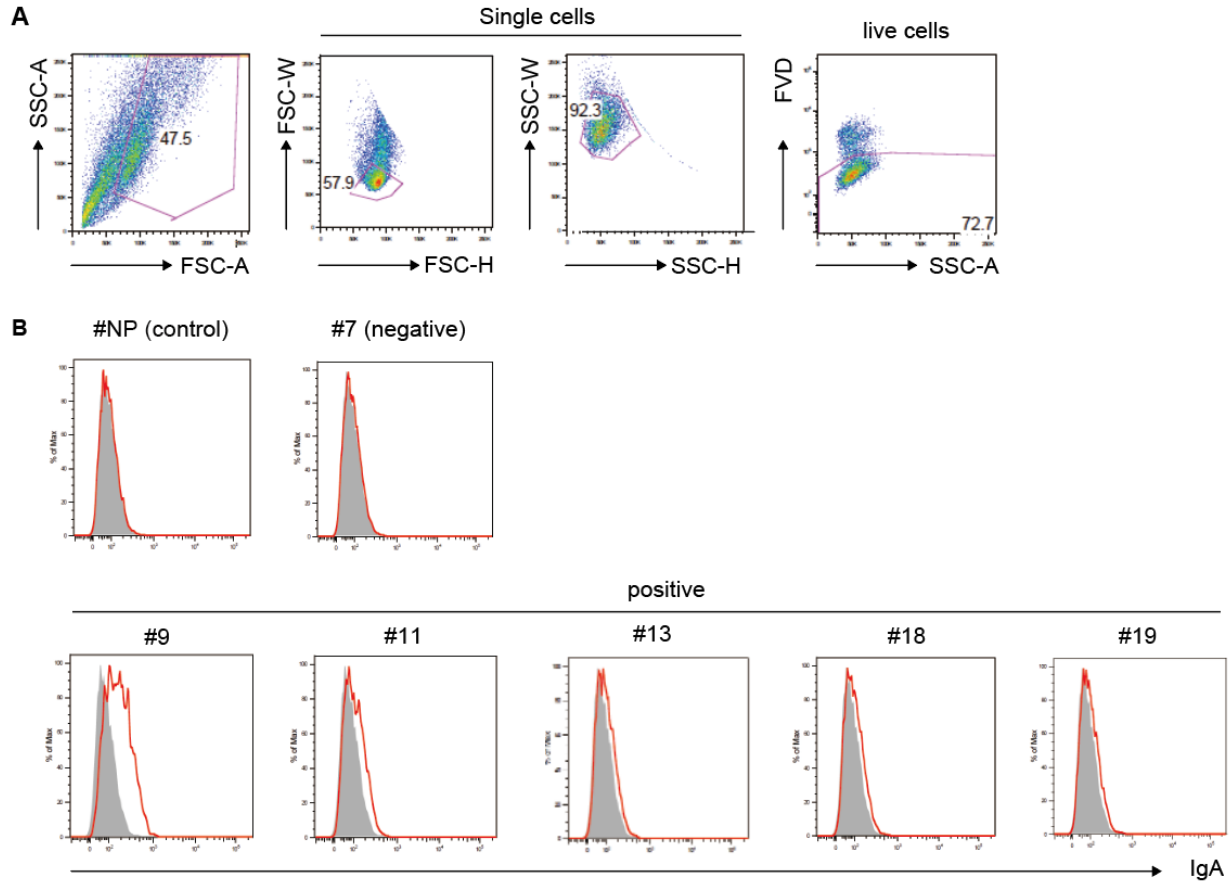


Fig. S9. MC binding of rIgAs generated from kidney IgA⁺ PBs of gddY mice

(A) Gating strategy for the flow cytometric analysis (Fig. 5B and fig. S9B) of primary-cultured mouse MCs.

(B) The MCs were intracellularly stained with the indicated rIgA Abs derived from IgA⁺ PBs in gddY mouse kidneys or anti-NP rIgA (#NP) (red line), or without the primary Ab (shaded), followed by anti-IgA Ab. Data are from the same experiment as shown in Fig. 5B.

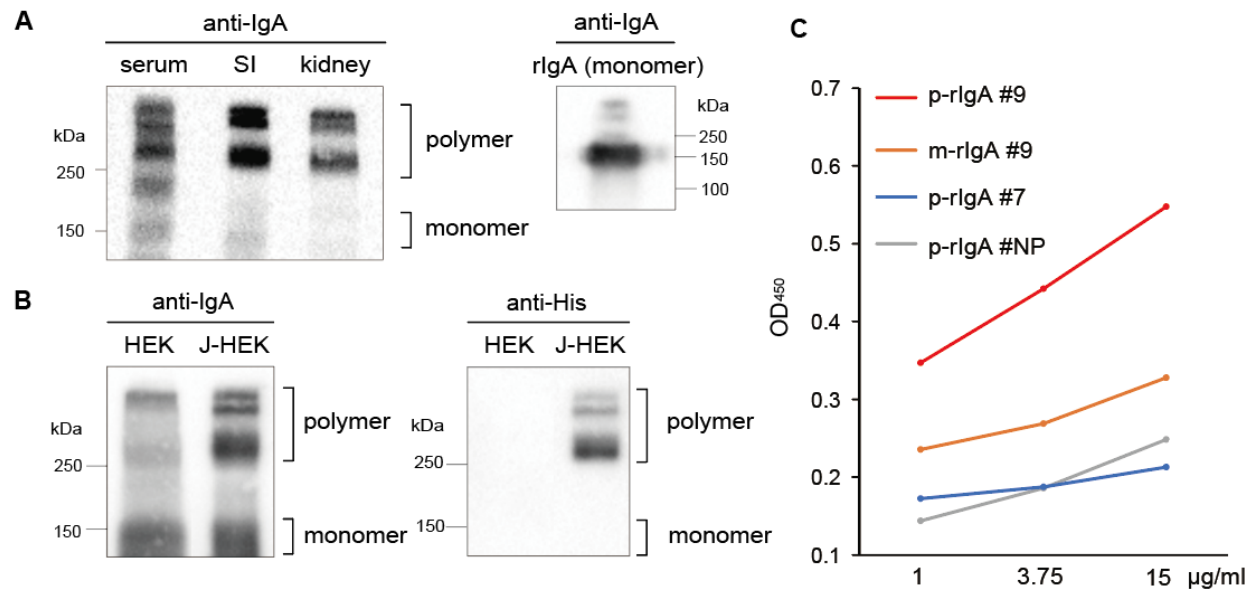


Fig. S10. Generation of polymeric rIgA derived from kidney IgA⁺ PBs of gddY mice

(A) Pooled sera from three gddY mice (serum) or supernatants of IgA⁺ ASCs from the small intestine (SI) or the kidney (kidney) of the same mice cultured for one day without any cytokines (left panel) and rIgA #9 (right panel) were subjected to SDS-PAGE under non-reducing conditions and probed with anti-IgA.

(B) Recombinant IgAs secreted from HEK293T cells (HEK) or those expressing His-tagged J chain (J-HEK) were analyzed as in (A) (left panel) and re-probed with anti-His-tag Ab (right panel).

(C) Reactivity of the indicated monomeric (m-) or polymeric (p-) rIgAs with FL-Sptbn1 was evaluated by ELISA. OD₄₅₀ values of each rIgA at the indicated concentrations are shown.

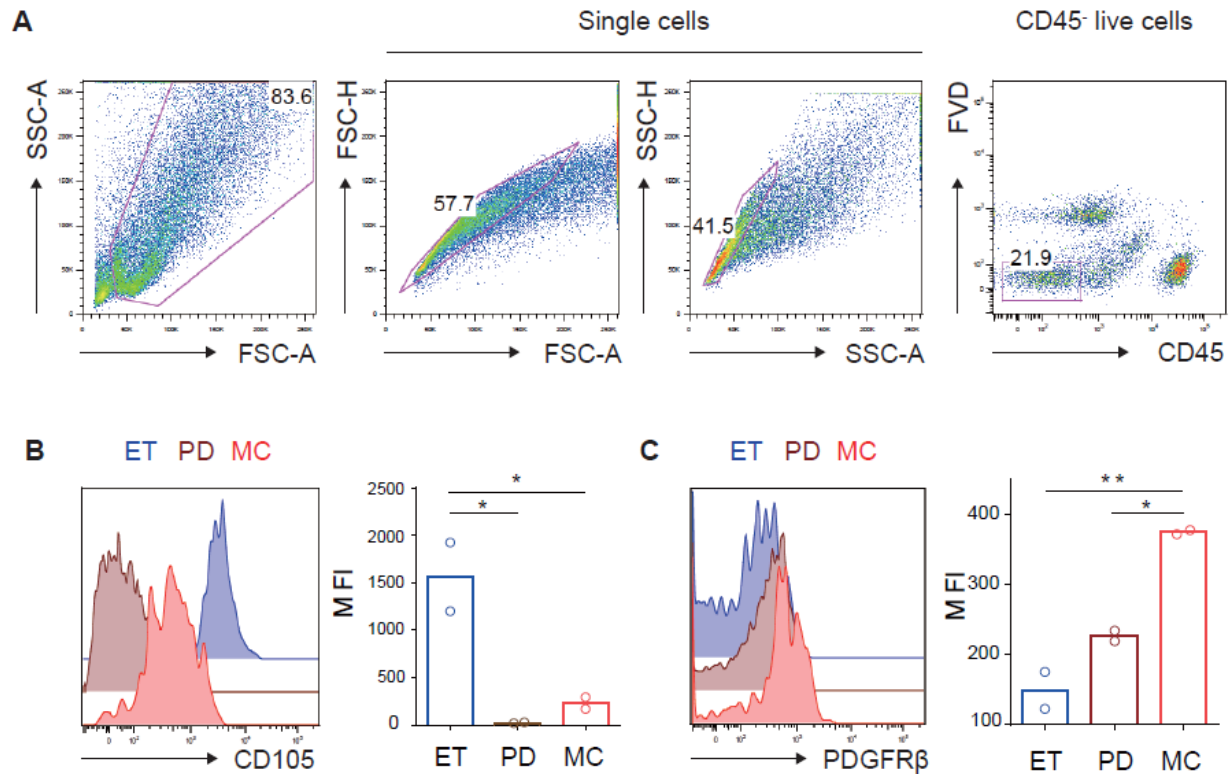


Fig. S11. Flow cytometric analysis of purified glomerular cells

(A to C) Flow cytometric analysis of combined glomerular cells collected from the kidneys of eight BALB/c mice.

(A) Gating strategy of non-leukocytes (CD45⁻) for (B and C) and Fig. 6A-C. The numbers indicate the percentage of gated cells (outlined) among the total cells plotted.

(B and C) Histograms showing CD105 (B) and PDGFR β (C) expression on the same ETs (blue), PDs (brown) or MCs (red) as shown in Fig. 6A-C. Average MFIs of CD105 or PDGFR β are shown as bar graphs (n=2). * $P < 0.05$, ** $P < 0.01$ (one-way ANOVA with multiple comparison test).

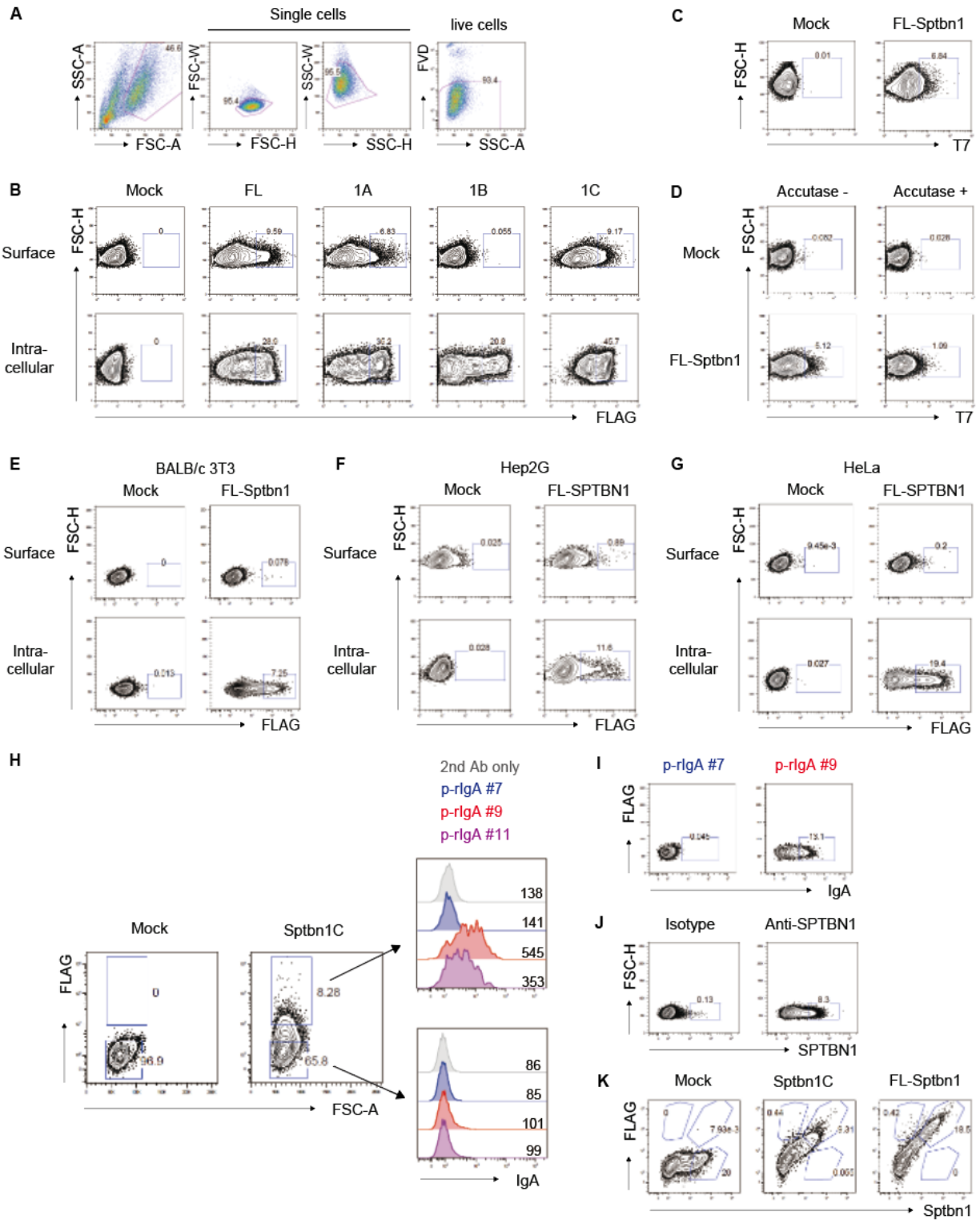


Fig. S12. Cell surface expression of β II-spectrin and its recognition by IgA auto-Abs of gddY mice

(A) Gating strategy for live cells analyzed by flow cytometry in (B to K) and Fig. 6D and E. The numbers indicate the percentage of the cells within the adjacent gates (outlined) among the total cells plotted.

(B to K) Flow cytometric analysis of the indicated cells transfected, or not, with the indicated expression vectors. The numbers indicate percentages of the cells within the gates among live cells.

(B) HEK293T cells transfected with mock, FLAG-tagged FL-Sptbn1 or Sptbn1A, 1B, or 1C vectors were stained with anti-FLAG Ab on the surface (top) or intracellularly (bottom).

(C) HEK293T cells transfected with mock or T7-tagged FL-Sptbn1 vectors were surface stained with anti-T7 Ab.

(D) HEK293T cells transfected as in (C) were treated with (right) or without (left) accutase for 10 min and then surface stained with anti-T7 Ab.

(E to G) BALB/c 3T3 cells transfected with mock or FLAG-tagged FL-Sptbn1 vectors (E), and Hep2G cells (F) or HeLa cells (G) transfected with mock or FLAG-tagged FL-SPTBN1 vectors, were analyzed as in (B).

(H) HEK293T cells transfected with mock or FLAG-Sptbn1C vectors were stained with anti-FLAG Ab and with or without the indicated p-rIgA Ab followed by the secondary anti-mouse IgA Ab. Surface binding of the secondary Ab on FLAG⁺ (upper gate) or FLAG⁻ (lower gate) live cells is shown as histograms with MFIs.

(I) HEK293T cells transfected with a mock vector were surface stained with p-rIgA #7 or #9, followed by anti-mouse IgA Ab.

(J) Untransfected HEK293T cells were surface stained with rabbit anti- β II-Spectrin Ab (right) or isotype-matched control Ab (left) followed by BV421-labelled anti-rabbit IgG Ab.

(K) HEK293T cells transfected with mock, FLAG-tagged Sptbn1C or FL-Sptbn1 vectors were surface stained with anti-FLAG and anti- β II-Spectrin Abs. All data are representative of two or three independent experiments.

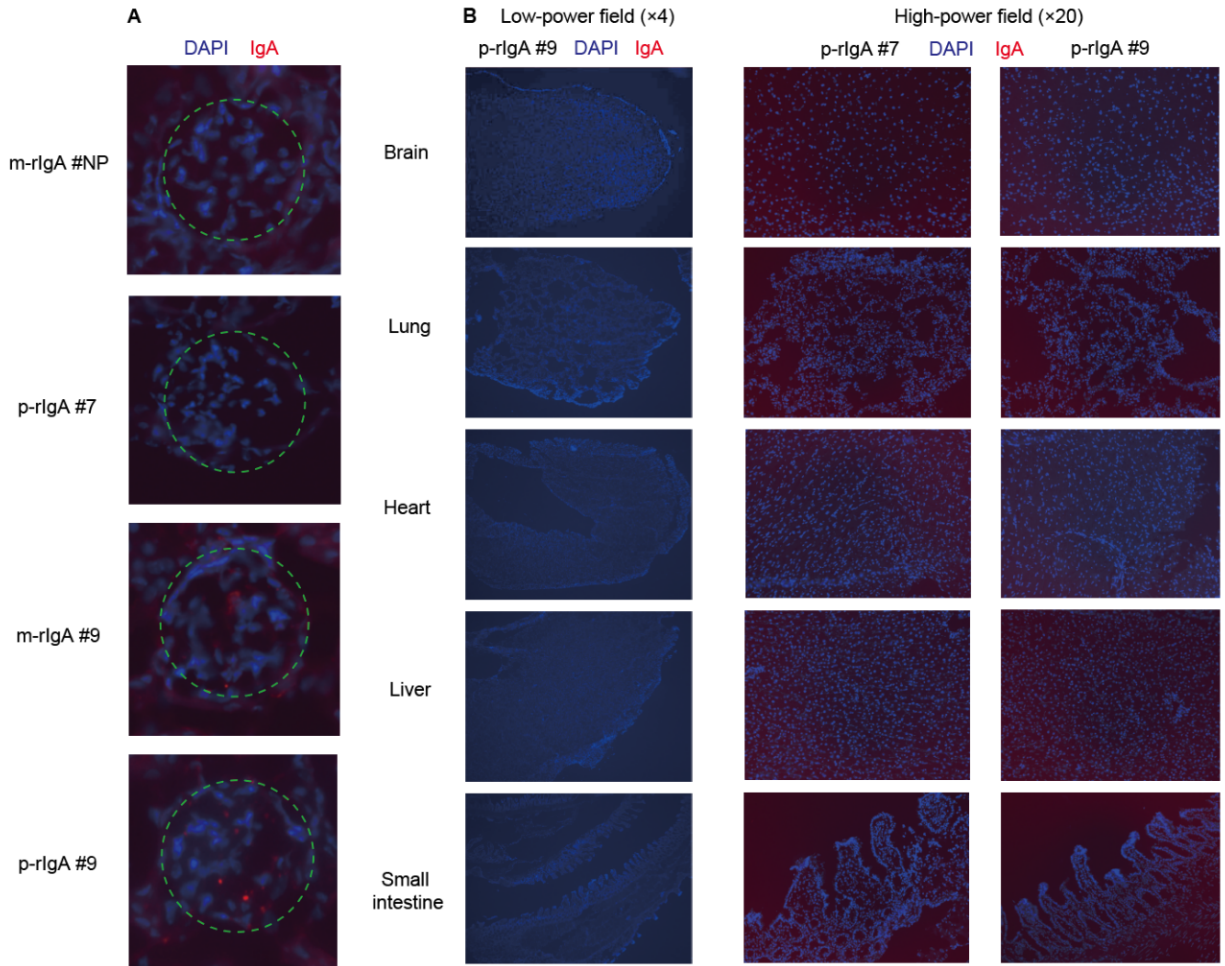


Fig. S13. Tissue specificity of *in vivo* binding by p-rIgA #9

(A) Immunofluorescence microscopy of sections of an AID-knockout mouse kidney, first stained with the indicated m-rIgA or p-rIgA Abs followed by PE-anti-IgA Ab (red) and DAPI (blue). The dashed circles represent areas of glomeruli.

(B) Sections of the indicated tissues from the same mice used in Fig. 6F and G (the mice injected with p-rIgA #7 or #9 as indicated) were stained with PE-anti-IgA Ab (red) and DAPI (blue). Data is one of two independent experiments with similar results.

rAb ID	V region (H)	D region (H)	J region (H)	Specific PCR primer (H, Fw)	Specific PCR primer (H, Rv)	V region (L)	J region (L)	Specific PCR primer (L, Fw)	Specific PCR primer (L, Rv)	No. amino acid mutation (H)	No. amino acid mutation (L)
1	IGHV1-19*01	IGHD5-2	IGHJ1*01	mVH8 Fw Xhol	mJH1 Rv NotI	IGKV5-39*01	IGKJ5*01	mVK11 Fw Xhol	mJK04 Rv NotI	6	2
2	IGHV1-18*01	IGHD2-1	IGHJ2*01	mVH8 Fw Xhol	mJH2 Rv NotI	IGKV6-13*01	IGKJ5*01	mVK11 Fw Xhol	mJK04 Rv NotI	9	6
3	IGHV5-17*01	IGHD2-4	IGHJ4*01	mVH6 Fw Xhol	mJH4 Rv NotI	IGKV4-61*01	IGKJ5*01	mVK3 Fw Xhol	mJK04 Rv NotI	4	10
4	IGHV5-12*01	IGHD2-14	IGHJ3*01	mVH19 Fw Xhol	mJH3 Rv NotI	IGKV6-15*01	IGKJ2*01	mVK11 Fw Xhol	mJK02 Rv NotI	4	14
5	IGHV1-12*01	IGHD4-1	IGHJ2*01	mVH23 Fw Xhol	mJH2 Rv NotI	IGKV1-110*02	IGKJ1*01	mVK15 Fw Xhol	mJK01 Rv NotI	1	4
6	IGHV6-3*01	IGHD1-1	IGHJ3*01	mVH5 Fw Xhol	mJH3 Rv NotI	IGKV4-54*01	IGKJ2*01	mVK3 Fw Xhol	mJK02 Rv NotI	4	13
7	IGHV1-82*01	IGHD1-1	IGHJ2*01	mVH2 Fw Xhol	mJH2 Rv NotI	IGKV4-68*01	IGKJ2*01	mVK3 Fw Xhol	mJK02 Rv NotI	5	5
8	IGHV1-18*01	IGHD2-2	IGHJ2*01	mVH8 Fw Xhol	mJH2 Rv NotI	IGKV12-38*01	IGKJ1*01	mVK10 Fw Xhol	mJK01 Rv NotI	8	10
9	IGHV5-6*01	IGHD1-1	IGHJ2*01	mVH6 Fw Xhol	mJH2 Rv NotI	IGKV10-96*02	IGKJ1*01	mVK14 Fw Xhol	mJK01 Rv NotI	4	2
10	IGHV1-19*01	IGHD2-4*01	IGHJ4*01	mVH8 Fw Xhol	mJH4 Rv NotI	IGKV1-110*02	IGKJ1*01	mVK15 Fw Xhol	mJK01 Rv NotI	0	2
11	IGHV5-9*01	IGHD2-14*01	IGHJ4*01	mVH19 Fw Xhol	mJH4 Rv NotI	IGKV6-29*01	IGKJ2*01	mVK22 Fw Xhol	mJK02 Rv NotI	6	3
12	IGHV1-18*01	IGHD2-14*01	IGHJ3*01	mVH8 Fw Xhol	mJH3 Rv NotI	IGKV14-126*01	IGKJ2*01	mVK8 Fw Xhol	mJK02 Rv NotI	4	0
13	IGHV1-72*01	IGHD2-3*01	IGHJ4*01	mVH1 Fw Xhol	mJH4 Rv NotI	IGKV10-96*02	IGKJ1*01	mVK14 Fw Xhol	mJK01 Rv NotI	4	1
14	IGHV3-1*01	IGHD2-3*01	IGHJ2*01	mVH15 Fw Xhol	mJH2 Rv NotI	IGKV4-68*01	IGKJ5*01	mVK3 Fw Xhol	mJK04 Rv NotI	5	5
15	IGHV5-17*01	IGHD2-4*01	IGHJ4*01	mVH6 Fw Xhol	mJH4 Rv NotI	IGKV4-68*01	IGKJ5*01	mVK3 Fw Xhol	mJK04 Rv NotI	4	11
16	IGHV1-52*01	IGHD2-14*01	IGHJ4*01	mVH6 Fw Xhol	mJH4 Rv NotI	IGKV6-13*01	IGKJ5*01	mVK11 Fw Xhol	mJK04 Rv NotI	6	7
17	IGHV1-58*01	IGHD2-13*01	IGHJ2*01	mVH8 Fw Xhol	mJH2 Rv NotI	IGKV14-100*01	IGKJ1*01	mVK19 Fw Xhol	mJK01 Rv NotI	3	3
18	IGHV1-18*01	IGHD2-1*01	IGHJ2*01	mVH8 Fw Xhol	mJH2 Rv NotI	IGKV6-13*01	IGKJ2*01	mVK11 Fw Xhol	mJK02 Rv NotI	0	3
19	IGHV5-17*01	IGHD1-1*01	IGHJ1*01	mVH6 Fw Xhol	mJH1 Rv NotI	IGKV1-117*02	IGKJ4*01	mVK23 Fw Xhol	mJK03 Rv NotI	0	5
20	IGHV1-19*01	IGHD2-4*01	IGHJ4*01	mVH8 Fw Xhol	mJH4 Rv NotI	IGKV6-13*01	IGKJ4*01	mVK11 Fw Xhol	mJK03 Rv NotI	5	2

Table S1. Characteristics of rIgA Abs generated from the kidneys of gddY mice

Identities of the germline V, (D) and J segments constituting the variable regions of heavy (H) and light (L) chains. Specific primers used for PCR amplification of the variable regions and the number of amino-acid mutations in the translated variable regions of the H and L chains, are outlined for each rIgA (rAb ID).

	HC (n=14)	IgAN (n=45) for detecting serum auto-Abs	IgAN (n=35) for detecting IgA ASCs in kidney samples
Age	33.3 【27-35】	35.2 【18-65】	36.9 【20-68】
Gender (M/F)	8/6	21/24	16/19
Serum IgA (mg/dl)	151 【41-260】	313.0 【150-533】	319 【174-533】
Gd-IgA1(μg/ml)	4.2 【1.7-8.3】	6.74 【3.1-18.0】	6.2 【2.9-11.9】
eGFR (ml/min/1.73m ²)	n. m	86.2 【35.8-117.6】	84.8 【26.8-138.2】
Proteinuria (g/gCr)	n. d	0.62 【0.1-3.57】	0.67 【0.3-4.83】

Table S2. Clinical characteristics of the participants

Clinical information of the healthy control individuals (HC) and the patients with IgAN involved in this study. M/F: male/female; Gd-IgA1: Galactose-deficient IgA1; eGFR: estimated glomerular filtration rate; n. m: not measured; n. d: not detected.

For generation of rAb		
PCR step	Name	5'-3' sequence
Igh 1st PCR	Igh 1st PCR Fw	GGAATTTCGAGGTGCAGCTGCAGGAGTCTGG
	Igh 1st PCR Rv (Ca)	CCTATATTGGTGGCACTTGAAG
Igh 2nd PCR	Igh 2nd PCR Fw	GGAATTTCGAGGTGCAGCTGCAGGAGTCTGG
	Igh 2nd PCR Rv (Ca)	TAAGTGCTAATGAAGGAAAGCCGT
Igk 1st PCR	Igk 1st PCR Fw (mix)	TGCTGCTGCTCTGGGTTCCAG
		ATTWTCAGCTTCTGCTAATC
		TTTTGCTTTTCTGGATTYCAC
		TCGTGTTKCTSTGGTTGTCTG
		ATGGAATCACAGRCYCWGGT
		TCTTGTTGCTCTGGTTYCCAG
		CAGTTCCTGGGGCTCTTGTGTTC
		CTCACTAGCTCTTCTCCTC
Igk 1st PCR Rv (Ck)	TTGACATAGGTAGAAGGGTGGTAG	
Igk 2nd PCR	Igk 2nd PCR Fw	GAYATTGTGMTSACMCARWCTMCA
	Igk 2nd PCR Rv (IgjK 1,2,4,5)	GTGGTTCGACCTTTAGTTCGCCGGCGTAATA
		CTGGTTCGACCTTTATTTCCGCCGGCGTAATA
		CTGGTTCGACCTCGACTTCGCCGGCGTAATA
gddY Ca	Ca Fw NotI	ATAATGCGGCCGCGAGAAATCCACCATCTACCC
	Ca Rv NheI	ATAATGCTAGCTCAGTAGCAGATGCCATCTCCCT
Ck	Igk Fw NotI	ATAATGCGGCCGCGATGCTGCACCACTGTATCCA
	Igk Rv NheI	ATAATGCTAGCCTAACACTATTCTGTTGAAGC
Specific PCR	mVH1 Fw XhoI	ATAATCTCGAGTCAGGTGCAGCTGCAGCAGCCTGG
	mVH2 Fw XhoI	ATAATCTCGAGTCAGGTGCAGCTGCAGCAGTCTGG
	mVH5 Fw XhoI	ATAATCTCGAGTCAGGTGAAGCTGGAGGAGTCTGG
	mVH6 Fw XhoI	ATAATCTCGAGTCAGGTGCAGCTGGTGGAGTCTGG
	mVH8 Fw XhoI	ATAATCTCGAGTCAGGTGCAGCTGCAGCAGTCTGG
	mVH15 Fw XhoI	ATAATCTCGAGTCAGGTACAGCTTCAGGAGTCAGG
	mVH19 Fw XhoI	ATAATCTCGAGTCAGGTGATGCTGGTGGAGTCTGG
	mVH23 Fw XhoI	ATAATCTCGAGTCAGTTCAGCTGCAGCAGTCTGG
	mJH1 Rv NotI	ATAATGCGGCCGCTGAGGAGACTGTGAGAGTGG
	mJH2 Rv NotI	ATAATGCGGCCGCTGAGGAGACTGTGAGAGTGG
	mJH3 Rv NotI	ATAATGCGGCCGCTGAGGAGACTGTGAGAGTGG
	mJH4 Rv NotI	ATAATGCGGCCGCTGAGGAGACTGTGAGAGTGG
	mVk3 Fw XhoI	ATAATCTCGAGTCAAATTTCTCACCCAGTCTCCA
	mVk8 Fw XhoI	ATAATCTCGAGTGACATCAAGATGACCCAGTCTCCA
	mVk10 Fw XhoI	ATAATCTCGAGTGACATCCAGATGACTCAGTCTCCA
	mVk11 Fw XhoI	ATAATCTCGAGTGACATTTGATGACTCAGTCTC
	mVk14 Fw XhoI	ATAATCTCGAGTGATATCCAGATGACACAGACTACA
	mVk15 Fw XhoI	ATAATCTCGAGTGATGTTGTGATGACCCAACTCCA
	mVk19 Fw XhoI	ATAATCTCGAGTGACATCCTGATGACCCAACTCCA
	mVk22 Fw XhoI	ATAATCTCGAGTAACATTGTAATGACCCAACTCCCC
	mVk23 Fw XhoI	ATAATCTCGAGTGATGTTTTGATGACCCAACTCCA
	mJk01 Rv NotI	ATAATGCGGCCGCTTGTATTTCCAGCTTGGTG
	mJk02 Rv NotI	ATAATGCGGCCGCTTATTTCCAGCTTGGTC
	mJk03 Rv NotI	ATAATGCGGCCGCTTATTTCCAACTTTGTC
mJk04 Rv NotI	ATAATGCGGCCGCTTCACTCCAGCTTGGTC	

For generation of Sptbn1		
FLAG-Sptbn1A	Sptbn1A Fw EcoRI	ATAATGAATTCACGACCACGGTAGCCACAGACT
	Sptbn1A Rv XbaI	ATAATTCTAGATCAATCTTTATGCTTCTTGACCA
FLAG-Sptbn1B	Sptbn1B Fw EcoRI	ATAATGAATTCAGTAGCAGAAGAGATCACCACCT
	Sptbn1B Rv XbaI	ATAATTCTAGATCAGAGCCCCACAGCTGCTTCA
FLAG-Sptbn1C	Sptbn1C Fw EcoRI	ATAATGAATTCACCTATTGAGGAAACTGAGAAAC
	Sptbn1C Rv XbaI	ATAATTCTAGATCACTTCTTCTTCCGAAAAGGC
T7-FL-Sptbn1	Sptbn1 FL Fw NotI	ATAATGCGGCCGCAACGACCACGGTAGCCACAGA
	Sptbn1 FL Rv EcoRI	ATAATGAATTCACCTTCTTCTTCCGAAAAGGC
FLAG-Sptbn1C	Sptbn1C Fw NotI	ATAATGCGGCCGCGCTGAGAAGAGCCAGAAGCT
	Sptbn1C Rv XbaI	ATAATTCTAGATCAATTCACAAAGAGTGAGCGGG

For generation of J-chain		
His tagged J chain	J chain Fw EcoRI	ATAATGAATTCGCCACCATGAAGACCCACCTGCT
	J chain Rv XhoI	ATAATCTCGAGTCAGTGGTGTGATGGTGGTGCAGGGTAGCAAGA

Table S3. Primer information

Primer information for generating rIgA Abs, FLAG-tagged Sptbn1A-C and FL-Sptbn1, and a His-tagged mouse J chain.

Supplemental auxiliary files:

Raw data for the figures of this article (an Excel file).